



INTERNATIONAL JOURNAL OF RECENT TECHNOLOGY SCIENCE & MANAGEMENT

“Crack Detection In Beams Using Experimental Model Data And Finite Element Model”**Mayank Sharma¹, Vishal Soni²**¹M. Tech Scholar, Mechanical Engineering, Oriental Institute of Science & Technology Bhopal, (M.P.), India²Assistant Professor, Mechanical Engineering, Oriental Institute of Science & Technology Bhopal, (M.P.), India**ABSTRACT**

In this paper, an analytical, as well as experimental approach to the crack detection in cantilever beams by vibration analysis is established. An experimental setup is designed in which a cracked cantilever beam is excited by a hammer and the response is obtained using an accelerometer attached to the beam. To avoid non-linearity, it is assumed that the crack is always open. To identify the crack, contours of the normalized frequency in terms of the normalized crack depth and location are plotted. The intersection of contours with the constant modal natural frequency planes is used to relate the crack location and depth. A minimization approach is employed for identifying the cracked element within the cantilever beam. The proposed method is based on measured frequencies and mode shapes of the beam.

KEYWORDS : Crack detection; Vibration analysis; Cantilever beam; Finite element method

I. INTRODUCTION

In the literature, several studies dealing with the structural safety of beams, especially, crack detection by structural health monitoring are entertained. Studies based on structural health monitoring for crack detection deal with change in natural frequencies and mode shapes of the beam. One of the most common structural defect is the presence of a crack. Cracks are present in structures due to various reasons. The presence of a crack could not only cause a local variation in the stiffness but it could also affect the mechanical behavior of the entire structure to a considerable extent. Cracks may be caused by fatigue under service conditions as a result of the constrained fatigue strength. Cracks may also occur due to mechanical defects. Another group of cracks are initiated during the manufacturing processes. Generally they are small in sizes. Such small cracks tend to propagate because of fluctuating stresses. If these propagating cracks remain undetected and reach their critical size, a sudden structural failure may occur. That is why it is possible to use natural frequency measurements to detect cracks. In the present investigation a number of literatures published so far have been surveyed, reviewed and analyzed. Most of the researchers studied the effect of single crack on the dynamics of structures. The objective is to carry out vibration analysis on a cantilever beam with and without crack. The results obtained analytically are validated with the simulation results. In first phase of the work two transverse surface cracks are included in developing the analytical expressions in dynamic characteristics of structures. These cracks introduce the new boundary conditions for the structures at the crack locations. These new boundary conditions are derived from strain energy equation using Castigliano's theorem. Presence of crack also reduces stiffness of the structures which is derived from stiffness matrix. The detailed analysis of crack modeling and stiffness matrices are presented in subsequent sections. Euler-Bernoulli beam theory is used for the dynamic characteristics of

beams with transverse cracks. Modified boundary conditions due to the presence of crack have been used to find out the theoretical expressions for natural frequencies and mode shape for the beams.

II. CRACK MODEL DESCRIPTION

This section presents the approach adopted to build the theoretical model for measuring the modal characteristics i.e. natural frequencies and mode shapes of the cracked beam containing multiple transverse cracks for different relative crack depths and relative crack positions and undamaged beam structure. During the analysis of the theoretical results, it is observed that a noticeable change in the first three mode shapes have been marked at the vicinity of crack locations. The robustness of the proposed theoretical approach has been established by comparing the results with the experimental results.

2.1 Evaluation of local flexibility of the damaged beam under axial and bending loading

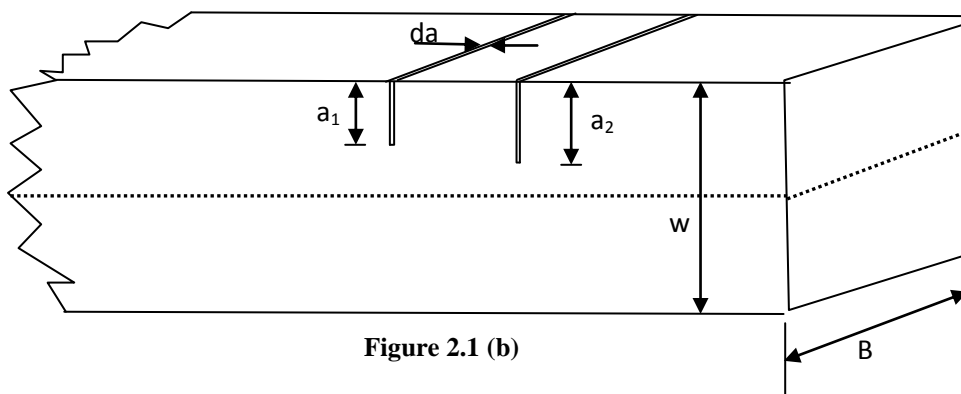
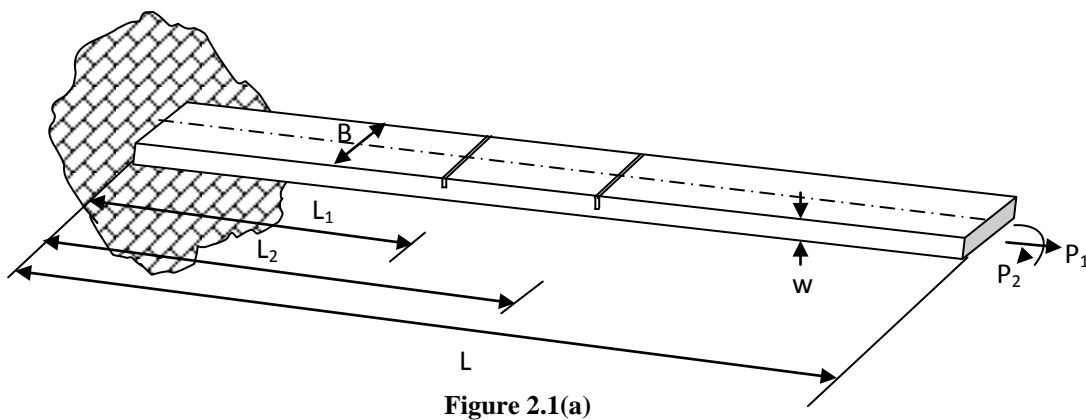


Fig. 2.1(a) presents a multi cracked cantilever beam, subjected to axial load (P_1) and bending moment (P_2). The loading provides a coupling effect resulting in both longitudinal and transverse motion of the beam. The beam contains two transverse cracks of depth ' a_1 ' and ' a_2 ' having width ' B ' and height ' W '. Due to the cracks present in the beam a local

flexibility will be introduced and a 2x2 matrix is considered, which represents the flexibility of the beam. Fig. 2.1(b) represents the cross sectional view of the cantilever beam model.

At the cracked section strain energy release rate can be explained as ;

$$J = \frac{1}{E'} (K_{I1} + K_{I2})^2 \quad \frac{1}{E'} = \frac{1-\nu^2}{E} \quad (2.1a)$$

$$= \frac{1}{E} \quad (\text{for plane stress condition}) \quad (2.1b)$$

The Stress intensity factors K_{I1} , K_{I2} are of mode I (opening of the crack) for load P_1 and P_2 respectively. The values of stress intensity factors from earlier studies [46] are;

$$\frac{P_1}{WB} \sqrt{\pi a} (F_1(\frac{a}{W})) = K_{I1}, \quad \frac{6P_2}{W^2B} \sqrt{\pi a} (F_2(\frac{a}{W})) = K_{I2}$$

$$F_1(\frac{a}{W}) = (\frac{2W}{\pi a} \tan(\frac{\pi a}{2W}))^{0.5} \left\{ \frac{0.752 + 2.02(a/W) + 0.37(1 - \sin(a\pi/2W))^3}{\cos(a\pi/2W)} \right\}$$

$$F_2(\frac{a}{W}) = (\frac{2W}{\pi a} \tan(\frac{\pi a}{2W}))^{0.5} \left\{ \frac{0.923 + 0.199(1 - \sin(a\pi/2W))^4}{\cos(a\pi/2W)} \right\}$$

Assuming U_t be the strain energy due to the crack. The additional displacement along the force P_i according to Castigliano's theorem is;

$$\frac{\partial U_t}{\partial P_i} = u_i \quad (2.4)$$

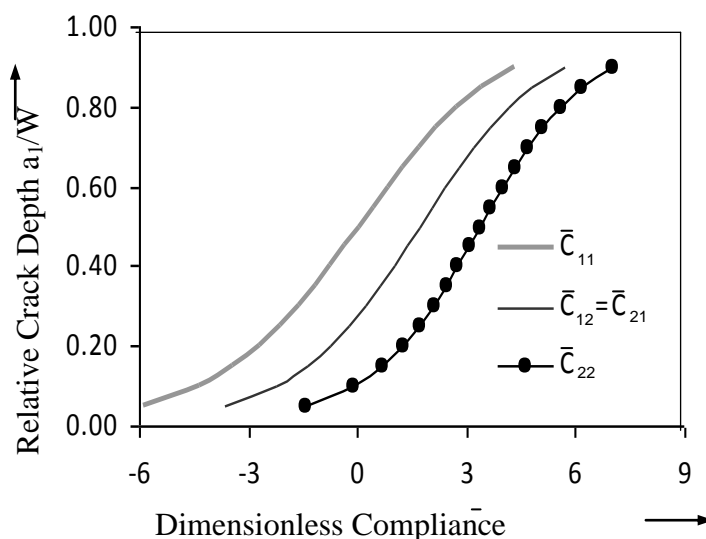


Fig. 2.2 Relative Crack Depth (a_1/W) vs. Dimensionless Compliance ($\ln(\bar{C}_{i=1,2,j=1,2})$)

The variations of dimensionless compliances with respect to relative crack depth have been shown in Fig. 2.2 and from the graph it is observed that the dimensionless compliance increases with increase in relative crack depths.

2.2 Vibration analysis of the multi cracked cantilever beam

In the present section, a cantilever beam (Fig. 2.3) with multiple crack with length 'L' width 'B' and depth 'W', having cracks at distance 'L₁' and 'L₂' with crack depths 'a₁' and 'a₂' respectively from the fixed end has been analyzed. The amplitudes of longitudinal vibration have been taken as u₁(x, t), u₂(x, t), u₃(x, t) and amplitudes of bending vibration have been considered as y₁(x, t), y₂(x, t), y₃(x, t) for the section-1(before 1st crack), section-2 (in between cracks), section-3 (after the 2nd crack) respectively as shown in Fig.3.4.

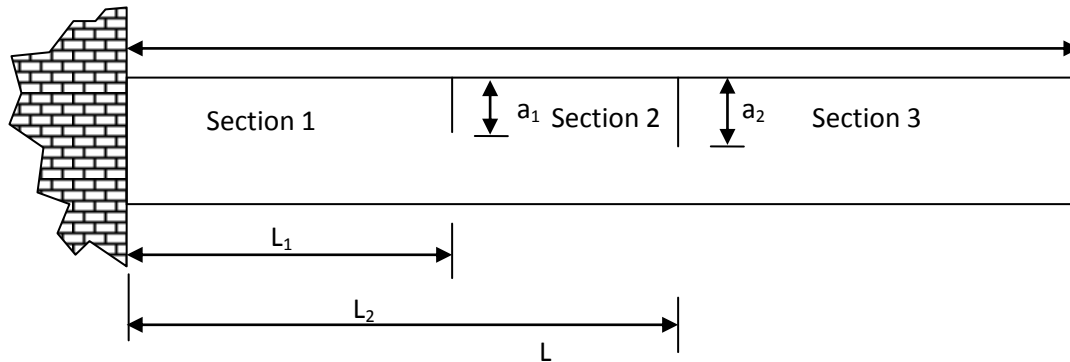


Fig. 2.3 Front view of the cracked cantilever beam

The following are the expressions of normal functions for the system

$$\bar{u}_1(\bar{x}) = A_1 \cos(\bar{K}_u \bar{x}) + A_2 \sin(\bar{K}_u \bar{x}) \quad (2.14a)$$

$$\bar{u}_2(\bar{x}) = A_3 \cos(\bar{K}_u \bar{x}) + A_4 \sin(\bar{K}_u \bar{x}) \quad (2.14b)$$

$$\bar{u}_3(\bar{x}) = A_5 \cos(\bar{K}_u \bar{x}) + A_6 \sin(\bar{K}_u \bar{x}) \quad (2.14c)$$

$$\bar{y}_1(\bar{x}) = A_7 \cosh(\bar{K}_y \bar{x}) + A_8 \sinh(\bar{K}_y \bar{x}) + A_9 \cos(\bar{K}_y \bar{x}) + A_{10} \sin(\bar{K}_y \bar{x}) \quad (2.14d)$$

$$\bar{y}_2(\bar{x}) = A_{11} \cosh(\bar{K}_y \bar{x}) + A_{12} \sinh(\bar{K}_y \bar{x}) + A_{13} \cos(\bar{K}_y \bar{x}) + A_{14} \sin(\bar{K}_y \bar{x}) \quad (2.14e)$$

$$\bar{y}_3(\bar{x}) = A_{15} \cosh(\bar{K}_y \bar{x}) + A_{16} \sinh(\bar{K}_y \bar{x}) + A_{17} \cos(\bar{K}_y \bar{x}) + A_{18} \sin(\bar{K}_y \bar{x}) \quad (2.14f)$$

Where, $\bar{x} = \frac{x}{L}$, $\bar{u} = \frac{u}{L}$, $\bar{y} = \frac{y}{L}$, $\beta_1 = \frac{L_1}{L}$, $\beta_2 = \frac{L_2}{L}$

$$\bar{K}_u = \frac{\omega L}{C_u}; \quad C_u = \left(\frac{E}{\rho} \right)^{1/2}; \quad \bar{K}_y = \left(\frac{\omega L^2}{C_y} \right)^{1/2}; \quad C_y = \left(\frac{EI}{\mu} \right)^{1/2}, \quad \mu = A\rho$$

The constants A_i , ($i=1, 18$) are to be calculated using the laid down boundary conditions.

The following are the boundary conditions for the cantilever beam;

$$\bar{u}_1(0)=0; \quad 2.15(a)$$

$$\bar{y}_1(0)=0; \quad 2.15(b)$$

$$\bar{y}'_1(0)=0; \quad 2.15(c)$$

$$\bar{u}'_3(1)=0; \quad 2.15(d)$$

$$\bar{y}''_3(1)=0; \quad 2.15(e)$$

$$\bar{y}'''_3(1)=0 \quad 2.15(f)$$

At the fractured section:

$$\bar{u}'_1(\beta)=\bar{u}'_2(\beta); \quad 2.16(a)$$

$$\bar{y}_1(\beta_1)=\bar{y}_2(\beta_1); \quad 2.16(b)$$

$$\bar{y}''_1(\beta_1)=\bar{y}''_2(\beta_1); \quad 2.16(c)$$

$$\bar{y}'''_1(\beta_1)=\bar{y}'''_2(\beta_1); \quad 2.16(d)$$

$$\bar{u}'_2(\beta_2)=\bar{u}'_3(\beta_2); \quad 2.16(e)$$

$$\bar{y}_2(\beta_2)=\bar{y}_3(\beta_2); \quad 2.16(f)$$

$$\bar{y}''_2(\beta_2)=\bar{y}''_3(\beta_2); \quad 2.16(g)$$

$$\bar{y}'''_2(\beta_2)=\bar{y}'''_3(\beta_2); \quad 2.16(h)$$

The expression in equation (3.17) can be found out because of the discontinuity of axial deformation to the right and left of the first crack location at the distance L_1 from the fixed end of the cantilever beam. Also at the cracked section, we have

$$AE \frac{du_1(L_1)}{dx} = k'_{11}(u_2(L_1) - u_1(L_1)) + k'_{12} \left(\frac{dy_2(L_1)}{dx} - \frac{dy_1(L_1)}{dx} \right) \quad (2.17)$$

Multiplying $\frac{AE}{Lk'_{11}k'_{12}}$ on both sides of equation (3.17) we get;

$$M_1 M_2 \bar{u}'_1(\beta_1) = M_2 (\bar{u}_2(\beta_1) - \bar{u}'_1(\beta_1)) + M_1 (\bar{y}'_2(\beta_1) - \bar{y}'_1(\beta_1)) \quad (2.18)$$

The expression in equation (2.19) can be found out because of the discontinuity of slope to the left and right of the crack at the crack section.

$$EI \frac{d^2 y_1(L_1)}{dx^2} = k'_{21} (u_2(L_1) - u_1(L_1)) + k'_{22} \left(\frac{dy_2(L_1)}{dx} - \frac{dy_1(L_1)}{dx} \right) \quad (2.19)$$

Multiplying $\frac{EI}{L^2 k'_{22} k'_{21}}$ on both sides of equation (2.19) we get;

$$M_3 M_4 \bar{y}''_1(\beta_1) = M_4 (\bar{y}'_2(\beta_1) - \bar{y}'_1(\beta_1)) + M_3 (\bar{u}_2(\beta_1) - \bar{u}_1(\beta_1)) \quad (2.20)$$

Similarly considering the second crack we can have;

$$M_5 M_6 \bar{u}'_2(\beta_2) = M_6 (\bar{u}_3(\beta_2) - \bar{u}_2(\beta_2)) + M_5 (\bar{y}'_3(\beta_2) - \bar{y}'_2(\beta_2)) \quad (2.21)$$

$$M_7 M_8 \bar{y}''_2(\beta_2) = M_8 (\bar{y}'_3(\beta_2) - \bar{y}'_2(\beta_2)) + M_7 (\bar{u}_3(\beta_2) - \bar{u}_2(\beta_2)) \quad (2.22)$$

Where $M_1 = AE/(Lk'_{11})$, $M_2 = AE/k'_{12}$, $M_3 = EI/(Lk'_{22})$, $M_4 = EI/(L^2 k'_{21})$

$M_5 = AE/(Lk''_{22})$, $M_6 = AE/k''_{23}$, $M_7 = EI/(Lk''_{33})$, $M_8 = EI/(L^2 k''_{32})$

By using the normal functions, equation (2.14a) to equation (2.14f) with the laid down boundary conditions as mentioned above, the characteristic equation of the system can be expressed as;

$$|Q| = 0 \quad (2.23)$$

This determinant is a function of natural frequency (ω), the relative locations of the crack (β_1, β_2) and the local stiffness matrix (K) which in turn is a function of the relative crack depth ($a_1/W, a_2/W$).

Where Q is a 18x18 matrix and is expressed as

$$[Q] = \begin{bmatrix} 0 & 0 & 0 & 0 & 0 & 0 & 0 & 0 & 0 & 0 & 0 & 0 & 1 & 0 & 0 & 0 & 0 & 0 \\ 1 & 0 & 1 & 0 & 0 & 0 & 0 & 0 & 0 & 0 & 0 & 0 & 0 & 0 & 0 & 0 & 0 & 0 \\ 0 & 1 & 0 & 1 & 0 & 0 & 0 & 0 & 0 & 0 & 0 & 0 & 0 & 0 & 0 & 0 & 0 & 0 \\ 0 & 0 & 0 & 0 & 0 & 0 & 0 & 0 & 0 & 0 & 0 & 0 & 0 & 0 & 0 & 0 & -T_1 & T_2 \\ 0 & 0 & 0 & 0 & 0 & 0 & 0 & 0 & G_3 & G_4 & -G_7 & -G_8 & 0 & 0 & 0 & 0 & 0 & 0 \\ 0 & 0 & 0 & 0 & 0 & 0 & 0 & 0 & G_4 & G_3 & G_8 & -G_7 & 0 & 0 & 0 & 0 & 0 & 0 \\ 0 & 0 & 0 & 0 & 0 & 0 & 0 & 0 & 0 & 0 & 0 & 0 & -T_6 & T_5 & T_6 & -T_5 & 0 & 0 \\ G_1 & G_2 & G_5 & G_6 & -G_1 & -G_2 & -G_5 & -G_6 & 0 & 0 & 0 & 0 & 0 & 0 & 0 & 0 & 0 & 0 \\ G_1 & G_2 & -G_5 & -G_6 & -G_1 & -G_2 & G_5 & G_6 & 0 & 0 & 0 & 0 & 0 & 0 & 0 & 0 & 0 & 0 \\ G_2 & G_1 & G_6 & -G_5 & -G_2 & -G_1 & -G_6 & G_5 & 0 & 0 & 0 & 0 & 0 & 0 & 0 & 0 & 0 & 0 \\ 0 & 0 & 0 & 0 & 0 & 0 & 0 & 0 & 0 & 0 & 0 & 0 & 0 & 0 & -T_4 & T_3 & T_4 & -T_3 \\ 0 & 0 & 0 & 0 & G_9 & G_{10} & G_{11} & G_{12} & -G_9 & -G_{10} & -G_{11} & -G_{12} & 0 & 0 & 0 & 0 & 0 & 0 \\ 0 & 0 & 0 & 0 & G_9 & G_{10} & -G_{11} & -G_{12} & -G_9 & -G_{10} & G_{11} & G_{12} & 0 & 0 & 0 & 0 & 0 & 0 \\ 0 & 0 & 0 & 0 & G_{10} & G_9 & G_{12} & -G_{11} & -G_{10} & -G_9 & -G_{12} & G_{11} & 0 & 0 & 0 & 0 & 0 & 0 \\ -S_3 & -S_4 & S_5 & -S_6 & S_3 & S_4 & -S_5 & S_6 & 0 & 0 & 0 & 0 & S_1 & -S_2 & T_5 & T_6 & 0 & 0 \\ S_7 & S_8 & -S_9 & -S_{10} & -S_{11} & -S_{12} & S_{13} & -S_{14} & 0 & 0 & 0 & 0 & S_{15} & S_{16} & -S_{15} & -S_{16} & 0 & 0 \\ 0 & 0 & 0 & 0 & V_3 & V_4 & -V_5 & V_6 & -V_3 & -V_4 & V_5 & -V_6 & 0 & 0 & V_1 & V_2 & -T_3 & -T_4 \\ 0 & 0 & 0 & 0 & V_7 & V_8 & -V_9 & -V_{10} & -V_{11} & -V_{12} & V_{13} & -V_{14} & 0 & 0 & V_{15} & V_{16} & -V_{15} & -V_{16} \end{bmatrix}$$

(2.24)

Where;

$$T_1 = \sin \bar{k}_u, T_2 = \cos \bar{k}_u, T_3 = \cos(\bar{k}_u \beta_2), T_4 = \sin(\bar{k}_u \beta_2), T_5 = \cos(\bar{k}_u \beta_1), T_6 = \sin(\bar{k}_u \beta_1),$$

$$G_1 = \cosh(\bar{k}_y \beta_1), G_2 = \sinh(\bar{k}_y \beta_1), G_3 = \cosh(\bar{k}_y), G_4 = \sinh(\bar{k}_y), G_5 = \cos(\bar{k}_y \beta_1)$$

$$G_6 = \sin(\bar{k}_y \beta_1), G_7 = \cos(\bar{k}_y), G_8 = \sin(\bar{k}_y), G_9 = \cosh(\bar{k}_y \beta_2), G_{10} = \sinh(\bar{k}_y \beta_2),$$

$$G_{11} = \cos(\bar{k}_y \beta_2), G_{12} = \sin(\bar{k}_y \beta_2), M_1 = AE/(Lk'_{11}), M_2 = AE/k'_{12}, M_3 = EI/(Lk'_{22}),$$

$$M_4 = EI/(L^2 k'_{21}), M_{12} = M_1/M_2, M_{34} = M_3/M_4, S_1 = T_5 - M_1 \bar{k}_u T_6, S_2 = T_6 + M_1 \bar{k}_u T_5,$$

$$S_3 = M_{12} S_{11}, S_4 = M_{12} S_{12}, S_5 = M_{12} S_{13}, S_6 = M_{12} S_{14}, S_7 = M_3 \bar{k}_y^2 G_1 + S_{11}, S_8 = M_3 \bar{k}_y^2 G_2 + S_{12},$$

$$S_9 = M_3 \bar{k}_y^2 G_5 + S_{13}, S_{10} = M_3 \bar{k}_y^2 G_6 - S_{14}, S_{11} = \bar{k}_y G_2, S_{12} = \bar{k}_y G_1, S_{13} = \bar{k}_y G_6, S_{14} = \bar{k}_y G_5,$$

$$S_{15} = M_{34} T_5, S_{16} = M_{34} T_6, M_5 = AE/(Lk''_{22}), M_6 = AE/k''_{23}, M_7 = EI/(Lk''_{33}), M_8 = EI/(L^2 k''_{32}),$$

$$\begin{aligned}
M_{56} &= M_5 / M_6, \quad M_{78} = M_7 / M_8, \quad V_1 = T_3 - M_5 \bar{k}_u T_4, \quad V_2 = T_4 + M_5 \bar{k}_u T_3, \quad V_3 = M_{56} V_{11}, \quad V_4 = M_{56} V_{12}, \\
V_5 &= M_{56} V_{13}, \quad V_6 = M_{56} V_{14}, \quad V_7 = M_7 \bar{k}_y^2 G_9 + V_{11}, \quad V_8 = M_7 \bar{k}_y^2 G_{10} + V_{12}, \quad V_9 = M_7 \bar{k}_y^2 G_{11} + V_{13}, \\
V_{10} &= M_7 \bar{k}_y^2 G_{12} - V_{14}, \quad V_{11} = \bar{k}_y G_{10}, \quad V_{12} = \bar{k}_y G_9, \quad V_{13} = \bar{k}_y G_{12}, \quad V_{14} = \bar{k}_y G_{11}, \quad V_{15} = M_{78} T_3, \\
V_{16} &= M_{78} T_4
\end{aligned}$$

III. CRACK DETECTION

Detection of crack in a beam is performed in two steps. First, the finite element model of the cracked cantilever beam is established. The beam is discretized into a number of elements, and the crack position is assumed to be in each of the elements. Next, for each position of the crack in each element, depth of the crack is varied. Modal analysis for each position and depth is then performed to find the natural frequencies of the beam. Using these results, a class of three dimensional surfaces is constructed for the first three modes of vibration, which indicate natural frequencies in terms of the dimensionless crack depth and crack position.

3.1 Finite element Analysis

The finite element analysis is a useful numerical technique that utilizes variation and interpolation methods for modeling and solving boundary value problems such as the one described in this current chapter. The finite element analysis is very systematic and can be useful for model with complex shape. So, the finite element model can be suitably employed for solving vibration based problems with different boundary conditions. Commercial finite element packages are available to address the practical problems. During finite element analysis, the structure is approximated in two ways. First step devotes to dividing the structure into a number of small parts. The small parts are known as finite elements and the procedure adopted to divide the structure is called as discretization. Each element on the structure has usually associated with equation of motion and that can be easily approximated. The each element on the finite element model has end points, they are known as nodes. The nodes are used to connect one element to other. Collectively the finite element and nodes are called as finite element mesh or finite element grid. In the second stage of approximation the equation of vibration for each finite element is determined and solved. The solution for each finite element brought together to generate the global mass and stiffness matrices describing the vibrational response of the whole structure. The displacement associated with the solution represents the motion of the nodes of the finite element mesh. This global mass and stiffness matrices represent the lumped parameter approximation of the structure and can be analyzed to obtain natural frequencies and mode shapes of damaged vibrating structures.

3.2 Modeling and Simulation in ANSYS

The finite element analysis is brought out for the cracked cantilever beam shown in fig 3.1 to locate the mode shape of transverse vibration at different crack depth and crack location. The dimensions of the cracked beams of the current research are as follows.

Length of the Beam (L) = 800mm;

Width of the beam (W) = 38 mm;

Thickness of the Beam (H) = 6mm;

Relative crack depth ($\zeta_1 = a_1/H$) = Varies from 0.25 to 0.5;

Relative crack depth ($\zeta_2 = a_2/H$) = Varies from 0.25 to 0.5;

Relative crack location ($\beta_1 = L_1/L$) = Varies from 0.625 to 0.875;

Relative crack location ($\beta_2 = L_2/L$) = Varies from 0.125 to 0.9375.

Properties for material in analysis:

Young's modulus= $E=70\text{GPa}$, Poisson's ratio= $\nu=0.35$, Density= $\rho=2.7\text{gm/cc}$

The finite element software ANSYS is used to the finite element analysis in the frequency domain and to get natural frequencies, and mode shapes.

A higher order 3-D, 10-node element having 3 degrees of freedom at each node: translations in the nodal x, y, and z directions (Specified as SOLID187 in ANSYS) shown in fig3.1 was selected based on concurrence study and used throughout the analysis. Each node has three degrees of freedom, making a total thirty degrees of freedom per element. Hexa meshed model, and meshing at vicinity of crack are exposed in fig 3.2, fig 3.3 respectively.

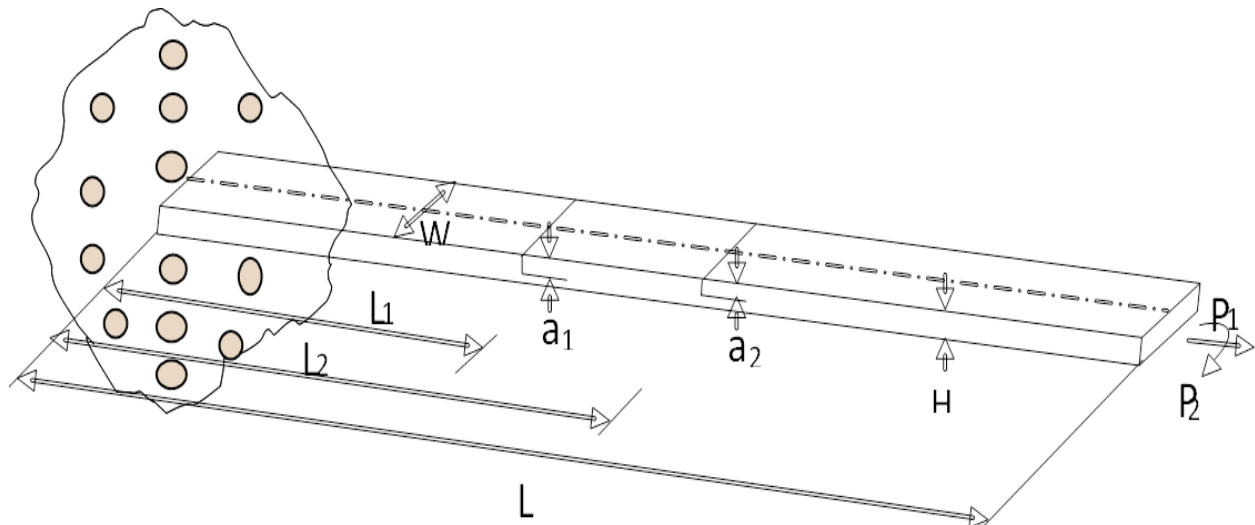


Fig. 3.2 Geometry Cantilever beam with multiple cracks

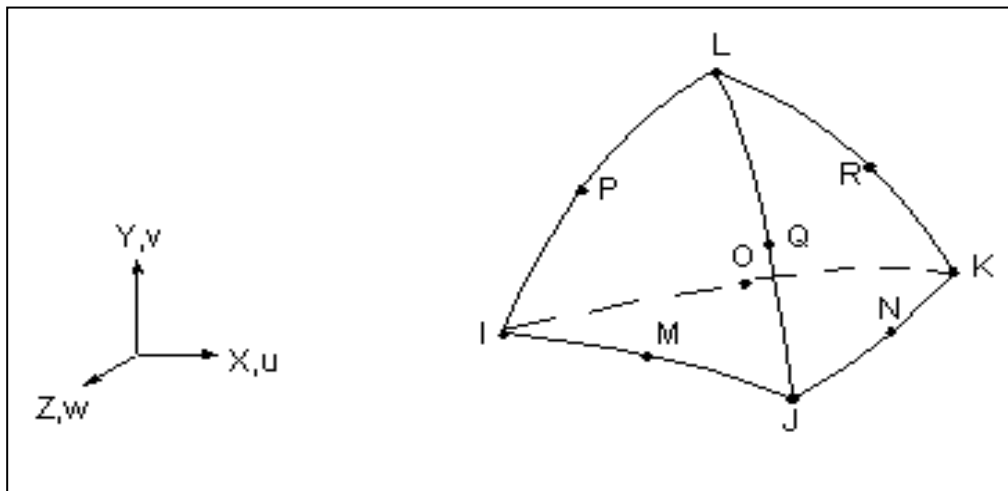


Fig. 3.3 SOLID187, element

Table1. Comparison of theoretical and numerical results

S No	Relative Crack Location and Position	Relative Natural Frequency					
		Theoretical Results			Numerical Results		
		I	II	III	I	II	III
1	$\varsigma_1=0.25; \varsigma_2=0.25;$ $\beta_1=0.125; \beta_2=0.1875$	0.007327	0.04815	0.1345	0.007687	0.04845	0.1357
2	$\varsigma_1=0.25; \varsigma_2=0.3;$ $\beta_1=0.25; \beta_2=0.3125$	0.00721	0.04811	0.1339	0.007679	0.04844	0.1347
3	$\varsigma_1=0.3; \varsigma_2=0.4;$ $\beta_1=0.3125; \beta_2=0.375$	0.00732	0.04765	0.1336	0.007663	0.04817	0.1341
4	$\varsigma_1=0.3; \varsigma_2=0.5;$ $\beta_1=0.4375; \beta_2=0.5$	0.00731	0.04672	0.1348	0.007678	0.04729	0.1354
5	$\varsigma_1=0.4; \varsigma_2=0.3;$ $\beta_1=0.5625; \beta_2=0.625$	0.00726	0.04714	0.1336	0.007716	0.04765	0.1346
6	$\varsigma_1=0.5; \varsigma_2=0.4;$ $\beta_1=0.625; \beta_2=0.6875$	0.00719	0.04713	0.1341	0.007728	0.04771	0.1349
7	$\varsigma_1=0.4; \varsigma_2=0.3;$ $\beta_1=0.75; \beta_2=0.8125$	0.00721	0.04779	0.1321	0.007744	0.04815	0.1325
8	$\varsigma_1=0.5; \varsigma_2=0.25;$ $\beta_1=0.875; \beta_2=0.9375$	0.00720	0.04811	0.1345	0.007754	0.04851	0.1353

Further the numerical investigation done so far must be validated with some theoretical or experimental results. In the present work, all the numerical results obtained with the help of ANSYS software is validated with the theoretical existing values taken from previous work .The theoretical analysis used for present comparison is for a beam with single crack and is modified for double crack for present investigation by following the equation given by the authors. To compare it, the outputs of the present work together with theoretical results are reflected in the form of table, to show the authentication of the current investigation. It is clear from the table 1 that the values obtained by numerical investigation are in good agreement with the already existing theoretical values for all three different modes and for different crack depth with different

positioning of it. The slight variations in the values are because of the various assumptions taken during numerical analyses which are slight different from the assumption taken during theoretical analysis by the authors. So the present numerical investigation proves to be handy for such analysis of cracked beam, and it can be said that for evaluating the relative natural frequency and amplitude of the multi cracked beam numerical investigation gives sufficient information regarding the matter.

IV. CONCLUSION

Following conclusions are based on above discussions supported in the form of graphical and tabular representation.

1. The crack location and its size strongly influence the mode shapes and natural frequencies of the cracked structures. The noteworthy changes in mode shapes are observed near crack location.
2. The positions of the cracks in relation to each other affect significantly the changes in the natural frequencies vibrations in the case of an equal relative depth of the cracks. When the cracks are located near to each other, the change in the natural frequency tends to increase.
3. The natural frequency of the structure having single crack tends to merge when the crack location is shifted toward the free end for the cantilever. And for case having two cracks, when the distance between the cracks increases, the frequencies of the beam natural vibrations also tend to the natural vibration frequencies of a system with a single crack.
4. In the case of two cracks of different depths, the larger crack has the most significant effect on the natural vibration frequencies. This is evident for the first natural vibration of a cantilever beam. For further more modes of vibration this is not so clear, because the influence of a crack location at a node is negligible. These changes in mode shapes and natural frequencies will be advantageous in prediction of crack location and its intensity and can further be extended to any multi crack system.
5. Good agreement between theoretical and numerical results is observed.

REFERENCES

1. A D.Dimarogonas.P.F. Rizos "Identification of Crack location and magnitude in a cantilever beam from the vibration modes" Journal of sound and vibration (1989)138(3) page no. 381-388.
2. R.Ballarini and Y.Hsu "Three-dimensional stress intensity factor analysis of a surface crack in a high-speed bearing" International journal of fracture 46,(1989) page no.141-158.
3. R.Ruotolo and D.Storer "Harmonic analysis of the vibrations of a cantilevered beam with a closing Crack" (1995) page no.1057-1074.
4. T.G.Chondros and A.D Dimarogonas "A continuous crack beam vibration theory" Journal of sound and vibration (1998)215(1) page no.17-34.
5. Kisa M. and Brandon J., The Effects of closure of cracks on the dynamics of a cracked cantilever beam, Journal of Sound and Vibration, 238(1), (2000) page no.1-18
6. Patil D.P., Maiti S.K, Detection of multiple cracks using frequency measurements, Engineering Fracture Mechanics 70, (2002), page no.1553-1572
7. M.I.Friswell and J.E.T.Penny "crack modeling for structural health monitoring" sage publications (2002) page no.139-148
8. Kisa M. "Free vibration analysis of a cantilever composite beam with multiple cracks", Composites Science and Technology 64, (2003),page no.1391-1402.
9. Patil D.P., Maiti S.K., Experimental verification of a method of detection of multiple cracks in beams based on frequency measurements" Journal of Sound and Vibration 281,(2004), page no.439-451.

10. Ertugrul.Cam and SadettinSorhan “An analysis of cracked beam structure using impact echo method”(2004)NDT&E International 38, page no.368-373.
11. S. Loutridis, E. Douka and L.J. Hadjileontiadis, Forced vibration behaviour and crack detection of cracked beams using instantaneous frequency”, NDT&E International, 38, (2005), page no. 411–419.
12. BarisBinici, “Vibration of beams with multiple open cracks subjected to axial force”, Journal of Sound and Vibration 287, (2005), page no .277–295.
13. H.R. Oz and M T Das, “In a plane vibration of circular curved beams with a transverse open crack”, Mathematical and Computational applications, (2006)vol 11,page no. 1-10.